Luminescent coordination nanoparticles†

Nicolas Kerbellec,[a] Laure Catala,[b] Carole Daiguebonne,[a] Alexandre Gloter,[c] Odile Stephan,[c] Jean-Claude Bünzli,[d] Olivier Guillou[a] and Talal Mallah*[b]

Received (in Montpellier, France) 11th December 2007, Accepted 13th February 2008
First published as an Advance Article on the web 25th February 2008
DOI: 10.1039/b719146d

Water-soluble lanthanide-containing coordination nanoparticles with a size around 4–5 nm were prepared by the growth confinement of the $Tb_2(bdc)_3(H_2O)_4$ three-dimensional network using an organic polymer; the terbium- and the europium-based objects present intense luminescence that opens perspectives for their use in different applications.

During the past few years, luminescent lanthanide-containing nanoparticles have been the subject of intense research because of their potential applications in different domains such as optics, electroluminescent devices, biological labels... To date, most luminescent lanthanide-containing nanoparticles are obtained by doping non-active oxide-, fluoride-, vanadate- or phosphate-based nanoparticles with the active rare earth ion. Because of the nature of the host nanoparticle matrix, the synthetic route needs usually relatively high temperatures, typically >200 °C. Only in few cases, mild conditions could be used to produce water-soluble nanoparticles.[1,2] Typical useful nanoparticle sizes are in the range 5–10 nm.

Coordination nanoparticles, *i.e.* nanoparticles made from metal ions connected by organic ligands, with sizes lower than 6 nm have been, to date, developed mainly for the cyanide-bridged systems.[3–5] Very recently, coordination particles with sizes between 100 and 1000 nm were reported.[6–9] Stabilizing coordination nanoparticles with large bridging organic ligands at sizes lower than 10 nm has not been achieved yet and is still a challenge. In this letter, we demonstrate the possibility of stabilizing coordination nanoparticles with sizes below 10 nm. This opens the perspective of transposing the chemical and the physical behavior intrinsic to coordination systems at the nanoscale. Here, we present the growth control of the luminescent coordination network $Tb_2(bdc)_3(H_2O)_4$ (H_2bdc is 1,4-benzenedicarboxylic acid) reported by Yaghi and co-workers,[10] by using the confinement effect of the organic polymer poly(vinyl pyrrolidone) (PVP). PVP has indeed been used with success to restrain the growth of metallic nanoparticles,[11] and recently of the Prussian blue coordination network.[12] The choice of an already existing and well-characterized network is crucial in order to have a structural signature that can be compared to that of the nano-objects prepared. The $Tb_2(bdc)_3(H_2O)_4$ edifice presents luminescence properties in the solid state, mainly because the large metal–metal distances imposed by the organic ligand prevent detrimental concentration quenching. However, because of their insolubility such systems cannot be used for many applications, particularly in biology.[13,14] On the other hand, transforming these metal–organic coordination networks into luminescent coordination nanoparticles has the following advantages: (i) they can be prepared at room temperature (ii) their synthesis can be achieved in a single step, (iii) they may be soluble in water, (iv) our ability to reduce their size to less than a few nanometres allows full advantage to be taken of the nano-confinement of electronic states affecting photophysical properties (lifetime, energy transfer processes, crystal-field splitting).

The infra-red spectrum of the nanoparticles (powder, see experimental section) is dominated by the bands corresponding to PVP, however, the two characteristic bands assigned to the ν_{sym} and the ν_{asym} vibrations of the COO^- group are present at 1386 and 1495 cm^{-1}, respectively (Fig. S1†). The X-ray powder diffraction diagram corrected from the contribution of the organic polymer contains the main peaks of the bulk compound (Fig. S2†).

Dynamic light scattering measurements were performed on the solutions coming from different preparations before the recovering procedure with acetone and after re-dispersion. Typical sizes of 8–10 nm were found for the average hydrodynamic diameter. Since the organic polymer itself has such a dimension when dissolved in water, these measurements give an upper value for the Tb particles present within the polymer. In order to get a more precise idea of the size of the objects, high angle annular dark field (HAADF) images have been acquired using a scanning transmission electron microscope (STEM). STEM-HAADF techniques show primary Z contrast and thus the Tb atomic distributions (terbium atoms being the heaviest atoms of the nanoparticle) should appear white on the images.

STEM-HAADF images obtained with a spatial resolution of around 0.8 nm are gathered in Fig. 1 and allow the identification of assemblies of particles within the PVP with a size around 4 nanometres. The small size of the particles, and the relatively small amount of Tb atoms with respect to the organic polymer limit the observation of well-defined objects (Fig. 1). Thus in order to ensure that the contrast observed on

[a] *Sciences Chimiques de Rennes, Équipe "Matériaux Inorganiques: Chimie Douce et Réactivité", UMR CNRS-INSA 6226, INSA, 20 Avenue des buttes de Coësmes, 35043 Rennes, France*
[b] *Institut de Chimie Moléculaire et des Matériaux d'Orsay, CNRS, Université Paris-Sud 11, 91405 Orsay Cedex, France. E-mail: mallah@icmo.u-psud.fr*
[c] *Laboratoire de Physique des Solides, UMR CNRS 8502, Université Paris-Sud 11, 91405 Orsay Cedex, France*
[d] *École Polytechnique Fédérale de Lausanne, Laboratoire de Chimie Supramoléculaire des Lanthanides, BCH 1402, CH-1015 Lausanne, Switzerland*

† Electronic supplementary information (ESI) available: Infra-red spectra, X-ray powder diffraction diagrams, excitation and luminescence spectra of Eu-based nanoparticles (Fig. S1–S9). See DOI: 10.1039/b719146d

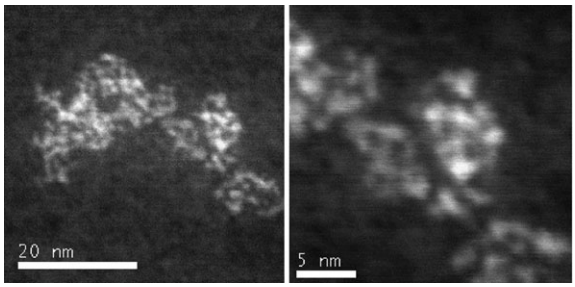

Fig. 1 STEM-HAADF images of the nanoparticles with two magnifications: left, scale bar 20 nm; right, scale bar 5 nm.

the images is due to the Tb nanoparticles, electron energy loss spectroscopy (EELS) was carried out. The right part of Fig. 2 shows the chemical images obtained with the EELS Tb $N_{4,5}$ edges (4d → 4f, energy window 147–177 eV) and is found to be superimposable with the STEM-HAADF image (Fig. 2, left) demonstrating that the small objects are indeed Tb-containing nanoparticles. EELS have also been performed at higher energy loss and the presence of Tb in the white contrasted particles has also been confirmed by the measurement of Tb $M_{4,5}$ edges (3d → 4f). EELS measurements were carried out on and between the particles. Between the particles of around 3–4 nm in size, the Tb N edge is not legible, demonstrating that

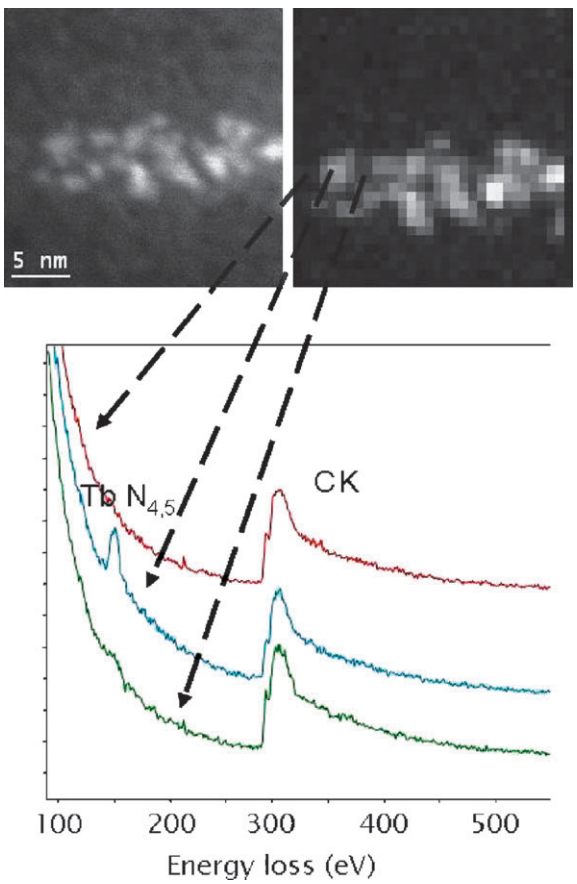

Fig. 2 Upper-left: STEM-HAADF image of the nanoparticles; upper-right: STEM-EELS image of the Tb (N edges); lower: three EELS spectra obtained at the positions noted on the STEM-EELS image; the peaks around 300 eV correspond to the C atoms K edge.

Tb-bearing nanoparticles are well separated. The C–K edges are detected all over the area since the particles are deposited onto an amorphous carbon grid. The typical length of a particle was estimated on a profile of STEM-HAADF images and an average of 3.1 nm with a standard deviation of 0.5 nm was found (from a sparse statistic of 32 particles).

Conventional transmission electron microscopy (TEM) imaging was also carried out. Unfortunately, images with a good contrast are difficult to observe and interpret because (i) the objects turned out to be unstable under the electron beam; this is a current problem encountered with some of the investigated nanoparticles having sizes lower than a few nanometres; (ii) the contrast is strongly damped by the poorly ordered thick polymer layer. Nevertheless, several bright field high resolution TEM images have been obtained at low temperature (liquid nitrogen sample holder, *ca.* 77 K) and confirm the crystallinity of these objects. (Fig. S3†).

The small size of the particles, combined with the low density of metal atoms stemming from their coordination nature, preclude the observation of well-defined images as expected for particles with high metal concentration (oxides, metallic...). Another way to characterize the objects present within the polymers is to explore their luminescent behavior. This was achieved by dispersing the particles in water and by exciting them at 312 nm (excitation spectrum of the Tb particles, Fig. S4†). The stability of the solution was checked prior to the study over a period of several weeks and no precipitation occurred. The characteristic $^5D_4 \rightarrow {}^7F_J$ transitions are detected in the visible range between 490 and 680 nm, with the hypersensitive $^5D_4 \rightarrow {}^7F_5$ transition (546 nm) being the most intense (Fig. 3). The quantum yield of the nanoparticles determined by Wrighton *et al.*'s method[15] amounts to 26.3 ± 2.2% and the Tb ($^5D_4$) lifetime is equal to 0.87 ± 0.05 ms. These values are very close to those found for 10 nm Tb-doped nanophosphors.[16] The luminescence decay of the excited states is single-exponential corresponding to a unique lifetime. This information will allow the proposal of a structural model for the nanoparticles (see below). Emission spectra of the nanoparticles were taken every hour for

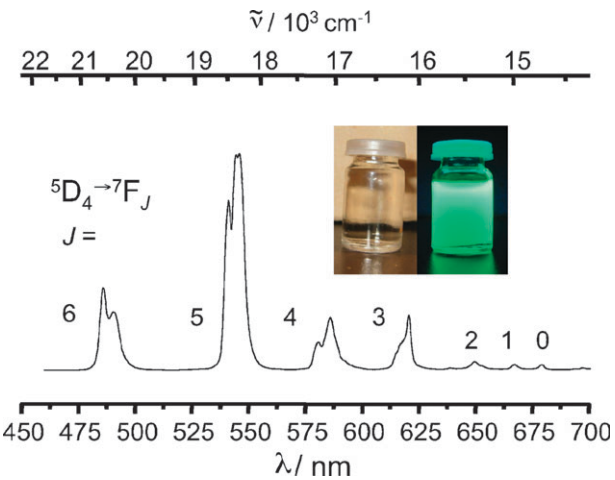

Fig. 3 Emission spectrum of the Tb nanoparticles re-dispersed in water and (inset) picture of the solution before and after irradiation at λ = 312 nm.

20 h without any change, which is consistent with a very good stability of the objects in solution.

The structure of the bulk compound $Tb_2(bdc)_3(H_2O)_4$ can be simply described as formed by layers of lanthanide ions connected by the oxygen atoms of the carboxylic groups with two different Tb–Tb distances of 5.0 and 6.1 Å; the layers are connected by the bdc^{2-} molecules that lie roughly perpendicular to the layers. Each Tb is surrounded by 6 bdc^{2-} ligands and 2 water molecules. The shortest Tb–Tb distance between two atoms belonging to two different layers is equal to 10.0 Å (1 nm) (Fig. S5 and S6†).[10] For a particle of 4–5 nm diameter more than 50% of the metal ions occupy the outer shell of the nanoparticle. These atoms are linked to the bdc^{2-} ligands that ensure their bridging to the Tb atoms belonging to the core of the particle. Their outer coordination sphere may be completed by (i) water molecules; (ii) oxygen atoms of the pyrrolidone units of PVP; (iii) bdc^{2-}, acting as terminal ligands; or (iv) a mixture of these possibilities. Since the photophysical studies lead to a unique lifetime for the excited states, one may safely assume that all the Tb atoms within the nanoparticles have a unique environment. This, on the one hand, excludes the assumption of a direct interaction between the PVP and the Tb atoms (the oxygen atoms of the organic ligands cannot be present in the coordination sphere of the Tb atoms) and on the other hand leads to the conclusion that the coordination sphere of the outer Tb atoms is exactly the same as for the core atoms surrounded by bdc^{2-} and water molecules (Fig. 4).

The lifetime of the Tb nanoparticles (0.87 ± 0.05 ms) is very close to that of the bulk compound (0.95 ± 0.03 ms). However, the quantum yield of the particles is almost half that of the bulk sample (26.3 compared to 43.5%). One possible hypothesis to explain this difference is the presence of water molecules in the surroundings of the particles trapped into the PVP polymer which may be responsible for a partial quenching of the ligand excited states through the vibrational energy of the OH groups. This is supported by the elemental analysis data (see above) that give 40 water molecules per unit formula. However, the particles remain sufficiently luminescent for potential applications.

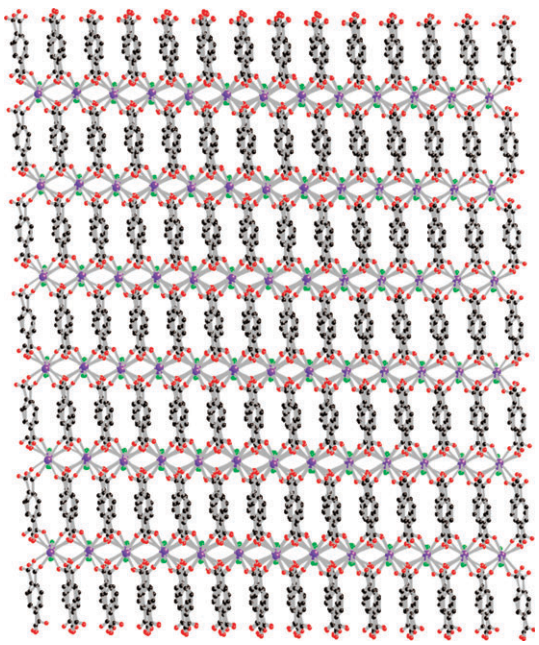

Fig. 4 Schematic view of a nanoparticle with Tb–Tb distances of $4.7 \times 4.7 \times 4.7$ nm showing the presence of terminal bdc^{2-}.

In this letter, we reported on the first luminescent nanoparticles obtained by the controlled growth of a 3-D coordination network that possess a size lower than 10 nm. We focused on Tb-based nanoparticles. However, it is possible to extend the synthesis to other lanthanides. Preliminary results confirm that Eu- and Er-based nanoparticles of the same coordination network can be prepared in PVP and re-dispersed in water. The Eu nanoparticles show, as expected, an intense red emission (Fig. S7–S9†). These results open the perspective of a room temperature one-step route to a large variety of luminescent nanoparticles in which chemists can control the spacing between the metal ions using adapted organic ligands. Furthermore, the size control below 10 nm will offer the possibility of application in biology that is generally difficult with larger objects.

The authors thank the Centre National de la Recherche Scientifique (CNRS), the French programme Nanoscience (ACI SupNanoMol NR0142), and the European community for financial support (Contract MRTN-CT-2003-504880/).

Experimental

Synthesis

A water solution containing Na_2bdc (0.164 g, 7.8×10^{-4} mol in 535 ml) is added to a mixture of $TbCl_3{\cdot}6H_2O$ (0.2 g, 5.36×10^{-4} mol) and PVP (5.8 g) dissolved in 535 ml of water. After one hour of stirring, a precipitate was recovered by the addition of acetone to the transparent solution and subsequently centrifuged. It was then dried under vacuum to afford a white powder. The latter was re-dispersible in water and in ethanol or methanol containing a small amount of water. Elemental analysis for $Tb_2(C_8H_4O_4)_3(H_2O)_{40}(C_6H_9NO)_{35}$, where C_6H_9NO corresponds to the formula of the monomer of the organic polymer PVP: experimental (calc.): %C: 51.8 (51.9); %H: 7.0 (7.4); %N: 9.3 (9.1); %O: 26.1 (25.7); Tb: 5.8 (5.9). The preparation of the Eu-based nanoparticles was carried out in the same way as above by using $EuCl_3{\cdot}6H_2O$.

Photophysics experiments

Broad-band excited emission spectra were recorded on a Fluorolog FL-3-22 spectrometer from Horiba-Jobin-Yvon Ltd; quartz cells with optical paths of 0.2 cm were used for room temperature spectra, while 77 K measurements were carried out on samples put into quartz Suprasil® capillaries. All spectra are corrected for the instrumental function. The quantum yields were determined by an absolute method[17] based on a home-modified integrating sphere from Oriel.[18] Lifetimes were measured on a previously described instrumental set-up[19,20] using a Nd-YAG laser equipped with frequency doubler, triplet and quadrupler, as well as with an OPO prism. Luminescence decays were single exponential functions.

Transmission electron microscopy

The scanning transmission electron microscopy (STEM) was carried out using a dedicated STEM-VG equipped with a cold field emission gun. Electron energy loss spectroscopy (EELS) was done using a CCD modified GATAN 666 PEELS. The STEM-EELS system then provides a spatial resolution of around 0.8 nm and an energy resolution at around 0.5 eV. High angle annular dark field images (HAADF) have been obtained on the same equipment where simultaneous STEM-EELS and STEM-HAADF is possible.

High resolution electron microscopy (HREM) has been obtained on a JEOL 2100 with a LN_2 cryo-sample holder.

References

1 A.-L. Pénard, T. Gacoin and J. P. Boilot, *Acc. Chem. Res.*, 2007, **40**, 895, and references cited therein.
2 S. W. Boettcher, J. Fan, C. K. Tsung, Q. Shi and G. D. Stucky, *Acc. Chem. Res.*, 2007, **40**, 784.
3 (*a*) L. Catala, T. Gacoin, J. P. Boilot, E. Rivière, C. Paulsen, E. Lhotel and T. Mallah, *Adv. Mater.*, 2003, **15**, 826; (*b*) L. Catala, A. Gloter, O. Stephan, G. Rogez and T. Mallah, *Chem. Commun.*, 2006, 1018.
4 Y. Guari, J. Larionova, K. Molvinger, B. Folch and C. Guerin, *Chem. Commun.*, 2006, 2613.
5 D. Brinzei, L. Catala, C. Mathoniere, W. Wernsdorfer, A. Gloter, O. Stephan and T. Mallah, *J. Am. Chem. Soc.*, 2007, **129**, 3778.
6 Y. M. Jeon, J. Heo and C. A. Mirkin, *J. Am. Chem. Soc.*, 2007, **129**, 7480.
7 W. J. Rieter, K. M. L. Taylor, H. Y. An, W. L. Lin and W. B. Lin, *J. Am. Chem. Soc.*, 2006, **128**, 9024.
8 Y. Sun, K. Ye, H. Zhang, J. Zhang, L. Zhao, B. Li, G. Yang, B. Yang, Y. Wang, S. W. Lai and C. M. Che, *Angew. Chem., Int. Ed.*, 2006, **45**, 5610.
9 M. Oh and C. A. Mirkin, *Nature*, 2005, **438**, 651.
10 T. M. Reineke, M. Eddaoudi, M. Fehr, D. Kelley and O. M. Yaghi, *J. Am. Chem. Soc.*, 1999, **121**, 1651.
11 J. Osuna, D. de Caro, C. Amiens, B. Chaudret, E. Snoeck, M. Respaud, J. M. Broto and A. Fert, *J. Phys. Chem.*, 1996, **100**, 14571.
12 T. Uemura and S. Kitagawa, *J. Am. Chem. Soc.*, 2003, **125**, 7814.
13 E. Beaurepaire, V. Buissette, M. P. Sauviat, D. Giaume, K. Lahlil, A. Mercuri, D. Casanova, A. Huignard, J. L. Martin, T. Gacoin, J. P. Boilot and A. Alexandrou, *Nano Lett.*, 2004, **4**, 2079.
14 D. Casanova, D. Giaume, T. Gacoin, J. P. Boilot and A. Alexandrou, *Biophys. J.*, 2007, 654A.
15 M. S. Wrighton, D. S. Ginley and D. L. Morse, *J. Phys. Chem.*, 1974, **78**, 2229.
16 V. Buissette, M. Moreau, T. Gacoin, J. P. Boilot, J. Y. Chane-Ching and T. Le Mercier, *Chem. Mater.*, 2004, **16**, 3767.
17 J. C. de Mello, H. F. Wittmann and R. H. Friend, *Adv. Mater.*, 1997, **9**, 230.
18 F. Gumy, *Patent application* 0013-066.B.WO, 2007.
19 R. Rodriguez-Cortinas, F. Avecilla, C. Platas-Iglesias, D. Imbert, J.-C. G. Bünzli, A. de Blas and T. Rodriguez-Blas, *Inorg. Chem.*, 2002, **41**, 5336.
20 A.-S. Chauvin, S. Comby, B. Song, C. D. B. Vandevyver, F. Thomas and J.-C. G. Bünzli, *Chem.–Eur. J.*, 2007, **13**, 9515.